Jpn. J. Appl. Phys. Vol. 37 (1998) pp. L 313–L 315
Part 2, No. 3B, 15 March 1998

Evolution of Surface Morphology and Strain in Low-Temperature AlN Grown by Plasma-Assisted Molecular Beam Epitaxy

Kyu-Hwan SHIM*[1], Jaemin MYOUNG, Oleg GLUSCHENKOV, Kyekyoon KIM*[2], Chinkyo KIM[1] and Ian K. ROBINSON[1]

Thin Film and Charged Particle Research Laboratory, Department of Electrical and Computer Engineering, University of Illinois at Urbana-Champaign, Urbana, Illinois 61801, USA

[1]*Department of Physics, University of Illinois at Urbana-Champaign, Urbana, Illinois 61801, USA*

(Received November 13, 1997; accepted for publication December 19, 1997)

The evolution of stress-driven surface roughening in low-temperature (LT) grown AlN has been investigated in a wide range of film thicknesses using plasma assisted molecular beam epitaxy and atomic force microscopy analysis. The relaxation of residual strain causing morphological instability after ∼50 nm thickness represents the kinetic stabilization of LT growth. LT-AlN layers with thicknesses of ∼20 nm provide excellent surface smoothness of <0.9 nm and large relaxation, ∼94% of the lattice mismatch strain. AlN films thicker than 50 nm, for which the scaling exponents are greater than 1, revealed stress-driven surface roughening with coherent islands. The implementation of thick LT-AlN buffer layers is limited by the stress-driven surface roughening above ∼50 nm thickness.

KEYWORDS: molecular beam epitaxy, AlN, plasma, morphology, strain

Group III-nitride semiconductors are promising materials for high-temperature and high-power microelectronics and ultra-violet/blue/green optoelectronics by virtue of their wide band gaps, high thermal conductivities and large electrical breakdown fields.[1–4] A low-temperature (LT) AlN nucleation layer grown on sapphire is designed to provide the GaN film with a smooth growth surface with reduced lattice mismatch.[5] The strain-induced transition of a planar two-dimensional (2D) AlN layer to a three-dimensional (3D) island morphology is a significant issue because the LT-AlN buffer layer serves as the crystallographic and morphological template for subsequent GaN growth. Recent works on surface morphology reported an improvement of the film quality after the annealing of LT-GaN and the nitridation of sapphire.[6,7] However, little is known about the evolution of the growing interfaces of AlN-sapphire heterostructures grown by plasma-assisted molecular beam epitaxy (PAMBE).

Interfaces grown under non-equilibrium conditions exhibit irregular geometries which can be analyzed in terms of the scaling properties of the surface fluctuations.[8,9] Theoretical works on the evolution of surface roughness have focused on the concept of dynamic scaling observing that growth can produce a self-affine surface.[10–13] The mean correlated height fluctuation G is defined over a length scale ρ parallel to the surface and the deposition time t at a given deposition rate, $G(\rho, t) = \langle [h(\rho_j, t) - h(\rho_i, t)]^2 \rangle^{1/2}$, where $h(\rho_j, t)$ and $h(\rho_i, t)$ are the heights of the surfaces at two locations labeled by ρ_j and ρ_i separated by a distance ρ. Self-affine growth results in a simple power-law scaling relationship for the surface roughness G as a function of the scaling exponent α and the growth exponent β. The dynamic scaling properties are given by $G \propto \rho^{\alpha}$ for $t_0 \ll t \ll t_s$, and $G \propto \rho^{\beta}$ for $t \gg t_s$, where t_0 and t_s are the characteristic time scales defining the initial transient time and the saturation time, respectively. Despite the many atomic models addressing surface roughening and growth kinetics, the evolution of the growth front is a subject of ongoing discussions due to the two different and competing kinetics of diffusion and the atomic desorption rate.

This work is designed to provide a detailed understanding of the surface roughening mechanisms of LT-AlN layers on sapphire over a wide range of film thicknesses. Discussions are focused on identifying and understanding the kinetic pathways to 3D growth of the strained heterostructures of LT-AlN on sapphire. This information is important to elucidate the strain relaxation mechanism and the interfacial properties, which contain relevant physics in a wide spectrum of the development of undulating topology in the AlN-sapphire system.

AlN samples were grown on the basal plane of a sapphire substrate at 550°C using PAMBE with 350-W rf power and 1-sccm nitrogen gas flow. The structural configuration and the growth processes of PAMBE have been described previously.[14] The surface of the substrate was examined using *in situ* 10-keV reflection high energy diffraction (RHEED) during the plasma cleaning of the substrate surface and the subsequent epitaxial growth procedure. Atomic force microscopy (AFM) analysis was performed with an ambient Topometrix system with silicon nitride cantilevers in contact mode. The scans were obtained with scan ranges of either 25 μm^2 with a tripod scanner or 1 μm^2 with a tube scanner at 400×400 points per scan. Root mean square (rms) roughness values were obtained from at least six different locations. Error ranges were obtained by calculating the standard deviation of the measurements from different areas of images.

RHEED patterns of AlN surfaces were taken along the $[11\bar{2}0]$ azimuth direction. The RHEED patterns were streaked due to a smooth surface as shown in Figs. 1(a) and 1(b) for 1.5 nm and 12 nm thick AlN films, and indicate a high crystalline quality of the epitaxial layers. However, the spotty pattern in Fig. 1(c) of the 140-nm-thick AlN film indicates that the surface undulation has occurred while the surface is maintained a single crystalline nature.

Shown in Fig. 2 is the rms roughness of LT-AlN epitaxial layers plotted as a function of film thickness. The observed initial surface of the sapphire substrate exhibited an rms roughness of ∼0.25 nm. The data in Fig. 2 present two separate regimes of film growth modes, one corresponding to a 2D planar growth with an rms roughness <1 nm and

*[1]On leave from Electronics and Telecommunications Research Institute.
*[2]Author to whom correspondence should be addressed. E-mail address: kevinkim@uiuc.edu

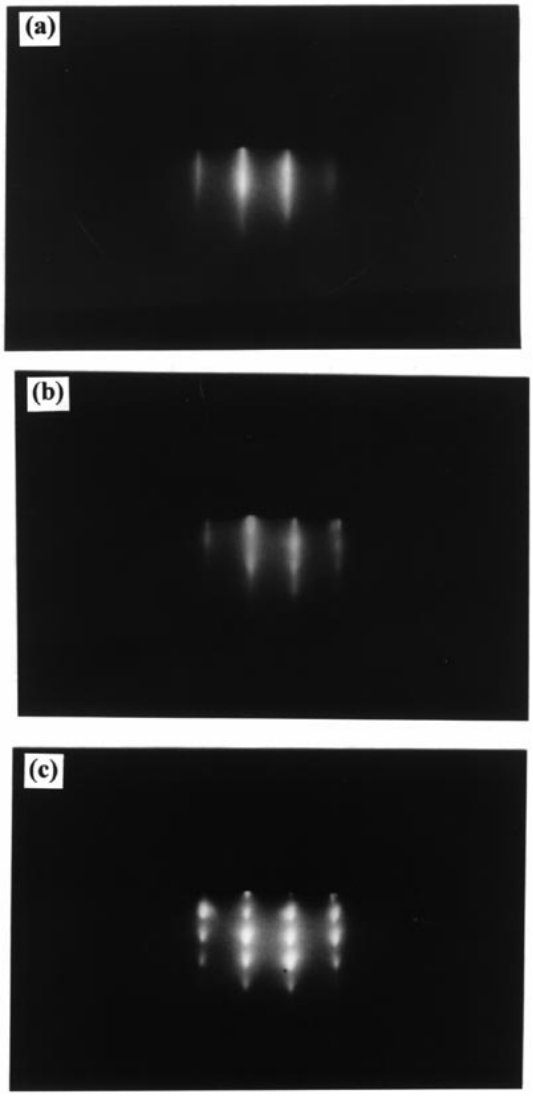

Fig. 1. RHEED patterns of AlN surfaces along the $[11\bar{2}0]$ azimuth direction during growth for the film thickness of (a) 1.5 nm, (b) 12 nm, and (c) 140 nm. Streak patterns in (a) and (b) represent a high crystalline quality of the epitaxial layers, and the spotty pattern in (c) represents the surface undulation, while the surface is maintains a single crystalline nature.

the other a transition to a very rough 3D growth at approximately 50-nm film-thickness, i.e., a Stranski-Krastanov (SK) mode growth. RHEED observations correspond very well to the surface undulation in the AFM images (data not shown). After the transient period of the relaxation process at ∼20–50 nm thickness, AlN films presented stress-driven surface roughening with coherent islands. The film of 140-nm thickness showed a high density of well-developed mounds with a large roughness of ∼6 nm. The average size of the crystallites could be measured from films thicker than 50 nm; the average size decreases from 300 nm to 80 nm as the films became thicker, from 50 nm to 140 nm.

The scaling exponents α of the AlN films with thicknesses of 22, 50, 140, and 270 nm as determined from 1D power spectrum density analysis are 0.6, 0.8, 1.0, and 1.5, respectively. The values of α in the range of 0.6–1.0 are within the predictions of diffusion-limited aggregation ($\alpha = 1$)[15] and MBE growth controlled by adsorption at kink sites ($\alpha = 0.66$),[10] while the large value, $\alpha = 1.5$, indicates faceted

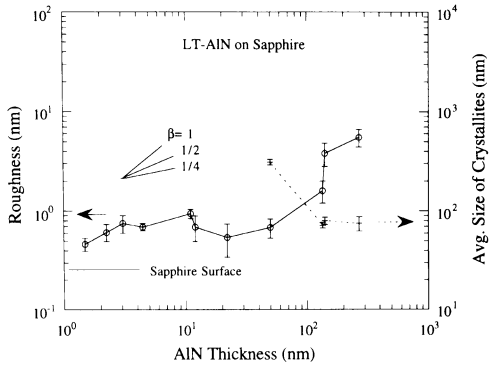

Fig. 2. The rms roughness and the average size of crystallites of LT-AlN films grown on sapphire substrates. The data show two separate regimes of film growth modes corresponding to 2D planar growth with an rms roughness <1 nm and a transition to very rough 3D growth at approximately 50 nm film thickness. The connection lines are to guide the eye.

growth.[16] The apparent scaling behavior exhibits a crossover from nonlinear (adsorption) to linear (diffusion) regimes and a transition to faceted growth of mounds. That is, the scaling exponents evidently present the panoramic evolution of growth modes in the strain-induced AlN from the 2D planar growth controlled by adsorption at the kink sites ($\alpha \sim 0.6$) to the stage of faceted growth ($\alpha \sim 1.5, \beta \sim 1$) with mounds. The roughness exponents at thin stages <10 nm are given by ($\alpha \sim 0.6, \beta \sim 1/2$), which agree very well with the theoretically determined values from a random-deposition (RD) model; ($\alpha = 1/2, \beta = 1/2$).[17] The exponents roughly satisfy a hyperscaling relationship of $\alpha + \alpha/\beta = 2$, which was predicted by the non-conservative models in which the formation of voids and overhangs and the desorption of deposited particles are allowed. Such behavior of Al adatoms on the film surface can be facilitated by the bombardment of energetic particles because thermal activation is extremely small at low temperatures.

The lattice constants of the thin AlN films were determined from X-ray measurements and a least-squares fit analysis as described previously.[5] The strain and lattice constants of AlN are plotted as a function of film thickness in Fig. 3, where the solid line represents a Matthew-Blakeslee (MB) model using cubic approximation.[18] The initial relaxation, 9.7% of the ultimate lattice mismatch and 11.7% between AlN ($a = 3.112$ Å) and sapphire ($a/\sqrt{3} = 2.747$ Å), represents the limit of plastic deformation, ∼2%, allowed at the interface between AlN and the sapphire substrate. LT-AlN layers with ∼20 nm thickness exhibit a surface roughness less than 0.9 nm and a compressive strain of ∼0.7%, which indicates that ∼94% of the lattice misfit strain was relaxed. The abrupt relaxation of strain after reaching ∼50 nm thickness is presumably due to the rapid dissipation of accumulated strain energy holding the highly undulated surface.

The critical thickness defining the instability for low-temperature dependence is theoretically estimated to be less than a monolayer thickness. However, the situation in the case of LT-AlN growth on sapphire appears to be different according to its featureless, smooth 2D planar growth to a relatively thick level of ∼20 nm. We propose three mechanisms to explain this extraordinary behavior of LT-AlN. The first and second mechanisms are the ion bombardment effect and the kinetic stabilization of LT growth, respectively. Both of these

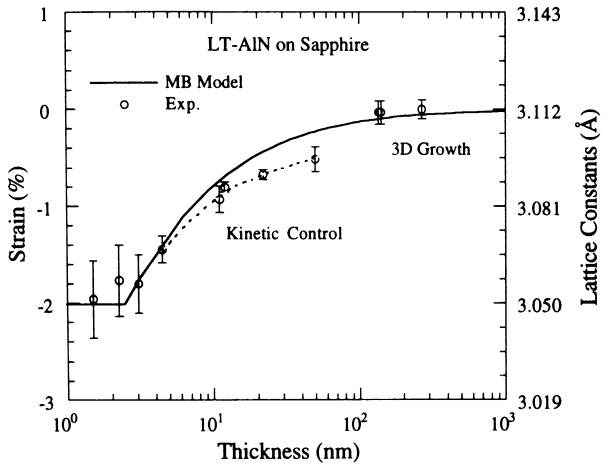

Fig. 3. The strain and the lattice constants of LT-AlN films grown on sapphire substrates. The solid line is calculated from a Matthew-Blakeslee model using cubic approximation.

mechanisms are believed to work together to prolong the 2D planar growth of AlN. The rf plasma, which supplies a flux of 1.4×10^{12} cm^{-2}·s^{-1} ions with ∼20-eV energy, may transfer sufficient kinetic energy to the growing film to suppress the island growth. The significance of the energetic particles in PAMBE will be discussed elsewhere in conjunction with the plasma parameters and the growth temperature. The third mechanism is the so-called magic lattice matching theorem, which has been developed to explain the pseudomorphic 2D growth of heterostructures with a large lattice mismatch. The strain in a magic lattice matched system which consists of a film with a lattice constant a_f and a substrate with a lattice constant a_s is given by $\varepsilon(m, n) = (ma_f - na_s)/ma_f$, where m and n are the number of unit lattices of the film and the substrate, respectively. In the AlN-sapphire system, the values of the strains corresponding to $(7, 8)$ and $(8, 9)$ leads to small compressive and tensile mismatches of 0.009 and 0.007, respectively. These plausible atomic arrangements do not exist in the GaN-sapphire system, in which a rough surface starts to appear at the initial stage of the growth. Moreover, the 2D nuclei mixed with the atomic arrangements of $(7, 8)$ and $(8, 9)$ can compensate for their reversal components, compressive and tensile, of the stresses. The 1:1 combination of $(7, 8)$:$(8, 9)$ structures may even lead to an extremely small residual strain, 0.0004. The reduced strain causes fewer defects at the initial stage of the film growth.

At present, there is no theory to predict the details of the roughening rate which is extremely rapid after a critical thickness. The important observation is that the morphological instability of AlN for the relaxation of the residual strain was postponed to ∼50 nm; the accumulated strain above static equilibrium experiences a rapid relaxation process. LT-AlN layers with ∼20 nm thickness provide excellent surface smoothness, <0.9 nm, and large relaxation, ∼94% of the lattice mismatch strain. On the contrary, the implementation of thick LT-AlN buffer layers to decrease stress driven roughening of subsequent films is limited by the rapid roughening above ∼50 nm thickness. Therefore, the film thickness <50 nm is considered to be most appropriate for application to nucleation layers for such subsequent films as GaN. The suppression of the stress-driven roughening, since it is kinetically controlled, might be further facilitated by lowering the substrate temperature and by increasing the growth rate. However, there will be other criteria for the critical thickness of the epitaxial growth, limited by the formation of an amorphous phase due to zero mobility of the surface adatoms at very low temperatures. At extremely low growth temperatures, the rf plasma parameters of PAMBE are expected to play a significant role in promoting the 2D planar growth.

In conclusion, we report, for the first time to our knowledge, an observation of kinetic stabilization significantly prolonging the 2D planar growth period of the Stranski-Krastanov mode for the LT-AlN films grown by PAMBE. The morphological instability of the LT-AlN film is suppressed up to ∼50 nm thickness; it provides excellent surface smoothness of <0.9 nm and large relaxation, ∼94% of the lattice mismatch strain, at ∼20 nm thickness. LT-AlN films thicker than 50 nm, for which the scaling exponents are greater than 1, experience stress-driven surface roughening with coherent 3D island growth. We propose the implementation of LT-AlN films with thicknesses below 50 nm to avoid rapid surface roughening and a transition to the 3D island growth.

Acknowledgements

One (K. H. Shim) of the authors would like to acknowledge Professor David G. Cahill for discussions and encouragement. This work was supported by the Physical Electronics Affiliates Program, the United States National Science Foundation (EED-8943166) through the Microelectronics Laboratory of the University of Illinois at Urbana-Champaign, and Samsung Electronics.

1) J. I. Pankove and E. R. Levin: J. Appl. Phys. **46** (1975) 1647.
2) S. Strite and H. Morkoc: J. Vac. Sci. & Technol. B **10** (1992) 1237.
3) H. Morkoc, S. Strite, G. B. Gao, M. E. Liu, B. Salverdlov and H. Burns: J. Appl. Phys. **5** (1994) 1363.
4) S. N. Mohammad, A. A. Salvador and H. Morkoc: IEEE Proc. **83** (1995) 1306.
5) C. Kim, I. K. Robinson, J. Myoung, K. H. Shim, M. C. Yoo and K. Kim: Appl. Phys. Lett. **69** (1996) 2358.
6) M. Yeadon, F. Hamdani, G. Y. Xu, A. Salvador, A. E. Botchkarev, J. M. Gibson and H. Morkoc: Appl. Phys. Lett. **70** (1997) 3023.
7) N. Grandjean, J. Massies, P. Vennegues, M. Laugt and M. Leroux: Appl. Phys. Lett. **70** (1997) 643.
8) N. E. Lee, D. G. Cahill and J. E. Greene: J. Appl. Phys. **80** (1996) 2199.
9) J. E. Van Nostrand, S. J. Chey, M. A. Hasan, D. G. Cahill and J. E. Greene: Phys. Rev. Lett. **74** (1995) 1127.
10) Z. W. Lai and S. D. Sarma: Phys. Rev. Lett. **66** (1991) 2348.
11) S. F. Edwards and D. R. Wilkinson: Proc. R. Soc. London A **381** (1982) 17.
12) F. Family: Physica (Amsterdam) **168A** (1990) 561.
13) M. Kardan, G. Parisi and Y. Zhang: Phys. Rev. Lett. **56** (1986) 889.
14) O. Gluschenkov, J. M. Myoung, K. H. Shim, K. Kim, Z. G. Figen, J. Gao and J. G. Eden: Appl. Phys. Lett. **70** (1997) 811.
15) D. E. Wolf and J. Villain: Europhys. Lett. **13** (1990) 389.
16) K. Fang, T. M. Lu and G. C. Wang: Phys. Rev. B **49** (1994) 833.
17) T. Viscek: *Fractal Growth Phenomena* (World Scientific, Singapore, 1989).
18) J. W. Matthews and A. E. Blakeslee: J. Cryst. Growth **27** (1974) 118.